Waves in Interplanetary Shocks: A Wind/WAVES Study

L. B. Wilson III, C. Cattell, P. J. Kellogg, K. Goetz, K. Kersten, L. Hanson, and R. MacGregor*
Department of Physics and Astronomy, University of Minnesota, Minneapolis, Minnesota 55455, USA

J. C. Kasper
Kavli Institute for Astrophysics and Space Research, Massachusetts Institute of Technology, Cambridge, Massachusetts 02139, USA
(Received 23 April 2007; published 26 July 2007)

We describe results from the first statistical study of waveform capture data during 67 interplanetary (IP) shocks with Mach numbers ranging from ~1–6. Most of the waveform captures and nearly 100% of the large amplitude waves were in the ramp region. Although solitary waves, Langmuir waves, and ion acoustic waves (IAWs) are all observed in the ramp region of the IP shocks, large amplitude IAWs dominate. The wave amplitude is correlated with the fast mode Mach number and with the shock strength. The observed waves produced anomalous resistivities from ~1–856 $\Omega \cdot$ m ($\sim 10^7$ times greater than classical estimates.) The results are consistent with theory suggesting IAWs provide the primary dissipation for low Mach number shocks.

DOI: 10.1103/PhysRevLett.99.041101 PACS numbers: 96.50.Fm, 52.35.Fp, 52.35.Tc, 96.50.Pw

Introduction.—Collisionless shock waves are a topic of considerable interest in space and laboratory plasma physics. In space, the usually high Mach number terrestrial bow shock has been extensively studied [1–5], but IP shocks are less well examined [6–9]. Wave data obtained at interplanetary shocks provide an excellent opportunity to study the role of wave dissipation at low Mach number shocks. A shock with a Mach number exceeding a theoretical critical Mach number (M_{cr}) may require, in addition to waves, mechanisms like ion reflection [10,11]. The often quoted $M_{cr} \approx 2.7$ is valid for a perpendicular shock (shock normal angle or $\theta_{Bn} = 90°$) propagating into a cold plasma. Accounting for θ_{Bn} and temperature, typical solar wind conditions will actually yield $M_{cr} \sim 1$–2 [10,11], values often observed in this study, suggesting particle reflection may occur even at these low Mach number shocks. However, since wave-particle interactions are thought to be the primary dissipation mechanism for these shocks [2,3,6–9,12], this study focuses on waves with $f_{pi} < f < f_{pe}$. Because of their role in particle acceleration [3,13,14] and energy dissipation in collisionless shocks [2,3,7,8,15–17], understanding the role of these waves in collisionless shocks is important in understanding the microphysics of IP shocks.

Three electrostatic (ES) wave modes are seen in this study of IP shocks: Langmuir waves, IAWs, and solitary waves. Langmuir waves have been studied extensively in the terrestrial foreshock and somewhat at IP shocks [1,5,6,9]. Langmuir waves are usually linearly polarized parallel to the ambient magnetic field with narrow frequency peaks near f_{pe}.

A number of authors [7,8,12,17] have concluded that IAWs are important in dissipating energy in lower Mach number shocks. Wave amplitudes in previous studies were found to be correlated with T_e/T_i [17,18]. They tend to be broadband bursty waves with Doppler shifted frequencies between 1–10 kHz (typically $f_{pi} < f < f_{pe}$) in the solar wind with a maximum intensity around 3 kHz [7,8,17]. They are usually linearly polarized close to parallel or oblique to the ambient magnetic field [19,20]. In a shock, the instability is thought to be driven by a relative drift between electrons and ions [18,21], with threshold drifts increasing for small T_e/T_i. A number of studies have concluded that IAWs are likely to be dominant in the terrestrial bow shock despite questions about high damping effects due to small T_e/T_i [19,20]. Theoretical studies suggest temperature gradients and oblique propagation of the waves can reduce damping when $T_e \sim T_i$.

Electrostatic solitary waves (ESWs) are characterized as nonlinear ES Debye-scale bipolar electric field signatures parallel to the ambient magnetic field [15,16,22–24], often associated with electron beams [16,22,23]. Solitary waves have been observed at the Earth's bow shock [2,3], and at an IP shock near ~8.7 AU [25], as well as within the magnetosphere at many boundaries [15,16,26] possibly providing energy dissipation. Simulations have shown them to form in and around the ramp regions of high Mach number collisionless shock waves [13,14].

Data sets and methodology.—The study presented herein investigated a 2 h window around the ramp region of 67 IP shocks with fast mode Mach number (M_f) ranging from ~1–6. This study focused on high frequency (typically $\geq$ 1 kHz) ES waves in the ramp region of IP shocks using the Wind/WAVES instrument [27]. It is worth noting, however, that waves exist below ~1 kHz [8] which are not accessible to study with a time domain sampler (TDS). Thirty-three of the 67 IP shocks had at least one waveform capture in the ramp region. The Wind satellite has a limited storage in the TDS buffer and a small percentage of the telemetry rate [27]. Were it to encounter ~1 min of very

large amplitude Langmuir waves upstream of an IP shock, it might not transmit any TDS samples from lower amplitude waves in the shock ramp itself due to an on board ranking system [27]. The WAVES instrument also has frequency domain receivers which allow one to look for waves possibly not seen in the TDS samples due to storage or sampling issues. Examination of the 34 events without ramp TDS samples using the WAVES thermal noise receiver (TNR) [27] showed a lower average wave power for frequencies ~4–10 kHz in these ramp regions compared to the 33 IP shocks with ramp TDS samples (recall IAWs typically have peak intensities near 3 kHz). There were no other noticeable differences between the 33 IP shocks with ramp TDS samples and the 34 without.

The waveforms were observed using a time TDS, which provides a ~17 ms waveform capture of 2048 points observed on two antennas sampled at 120 kHz (from here on, a waveform capture is called a TDS sample). Most of these shocks were quasiperpendicular. The ramp duration, or thickness, is defined as the duration from the point of lowest magnetic field immediately preceding the ramp to the point of highest magnetic field immediately following the ramp [28] using 3 s MFI data [29]. Typical ramp durations were from 3–10 s ($\lesssim 0.1\%$ of the total time studied per shock) with the average ramp duration ~8 s. We defined waves with $|E_{xy}| = \sqrt{E_x^2 + E_y^2} \geq 5$ mV/m as large ($|E_{xy}|$ is the *pk-pk E*-field amplitude in the plane of the ecliptic). Wave dependence on Mach numbers, shock strength, θ_{Bn}, as well as region of occurrence, wave type, and size were examined.

Figure 1 shows an example of a shock crossing on 10/10/1997. The shock arrival time was 15:57:07 UT. This shock had $M_f \sim 1.5$, $\theta_{\mathrm{Bn}} \sim 88°$, $n_2/n_1 \sim 1.6$ [30], and T_{e1}/T_{i1} [31,32] was ~0.8–1.0 in the upstream. There were 4 TDS samples in the ramp with an average $|E_{xy}|$ ~18 mV/m. The average number of TDS samples in the 33 IP shock ramps analyzed was ~3. Panel I is the electric field intensity (dB above background) in 1 min averages for 4–100 kHz (from the WAVES TNR instrument [27]). Emissions at the plasma frequency are clearly visible ranging from ~20–40 kHz with intensifications in the ramp. Intensification at IA frequencies (ranging from 4–10 kHz [7,17]) can be seen in the ramp (consistent with observed TDS samples). Langmuir waves are first seen at 15:56:58 UT (~ 6 seconds before ramp) in the TDS samples consistent with a localized increase around that same time near 30–40 kHz in panel I. Panel II plots the electron fluxes for energies of 9–1151 eV from the 3DP instrument [31]; panel III is a plot of T_e/T_i (3DP instrument); panel IV is the 3 s averaged magnetic field magnitude (nT) from the MFI instrument [29]; and panel V is the electron density (cm^{-3}) (also from the 3DP instrument).

Three TDS samples illustrating the 3 wave types observed in this study are shown on the right in Fig. 1. each wave is labeled with large red letters (Langmuir wave, A), (IAW, B), and (solitary wave, C). For the Langmuir and IAWs, the polarization with respect to the ambient magnetic field was also shown.

Results and discussion.—Table I summarizes the statistics on the waves in the upstream, ramp, and downstream regions for the 33 IP shocks. The last three rows were normalized by the average duration for their respective regions (up/downstream $\bar{\tau}_u = \bar{\tau}_d \simeq 3596$ s, and ramp $\bar{\tau}_r \simeq 8$ s), yielding a normalized percentage of occurrence per region. One can easily see the ramp region has the highest probability of wave occurrence. Roughly 87% of all the waves seen in the 33 IP shock ramps were IAWs and 90% of these were large (≥ 5 mV/m). The dominant wave mode upstream is large amplitude Langmuir waves (~ 53% of all the large waves upstream for the 33 shocks with ramp waves), consistent with other observations at IP shocks [6,9] and the terrestrial bow shock [1]. The downstream region is dominated by IAWs (~ 82% of all the downstream waves for the 33 IP shocks); however, ~68% of those were small IAWs. The dominant wave mode (for $f_{\mathrm{pi}} < f < f_{\mathrm{pe}}$) in the ramp region is large IAWs. The most striking observation is that essentially 100% of the large amplitude IAWs occur in the ramp when normalized by time, supporting theories on dissipation in low Mach number shocks [13,14].

Because of the high probability of occurrence for large amplitude IAWs in the ramp regions, the dependence of wave amplitude ($|E_{xy}|$) on various shock parameters

TABLE I. Wave occurrence by regions for the 33 IP shocks with ramp TDS samples.

	All waves			Large (≥ 5 mV/m)		
	Langmuir	Ion Acoustic	Solitary	Langmuir	Ion Acoustic	Solitary
# Up	52	102	20	33	28	1
# in Ramps	5	78	7	5	71	5
# Down	8	91	12	6	29	3
	Normalized Probability of Occurrence					
Up	2.3%	0.3%	0.6%	1.4%	0.1%	0.0%
Ramp	97.4%	99.5%	99.0%	98.3%	99.8%	99.8%
Down	0.3%	0.3%	0.4%	0.3%	0.1%	0.1%

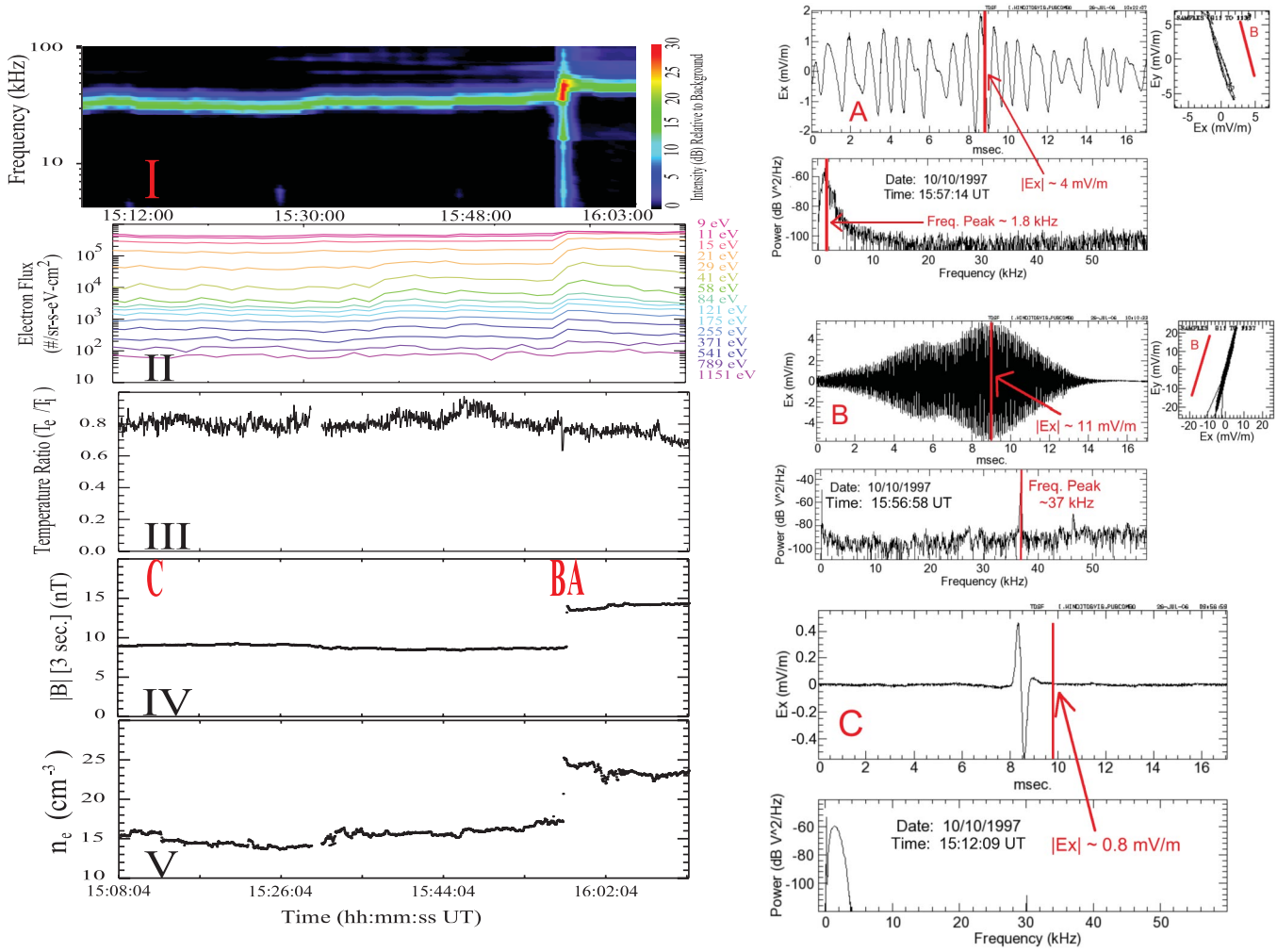

FIG. 1 (color). An example of a fast forward IP shock wave on 10/10/11997 [27,29,31]. Panels I–V present data from different Wind instruments. Panel IV labels the time of occurrence for each of the three wave types shown to the right with capital red letters (**A** = Langmuir, **B** = IA, and **C** = Solitary). An associated polarization plot is shown for the Langmuir and IAWs.

including: θ_{Bn}, n_2/n_1, M_a, M_f, M_{cs}, and T_e/T_i were tested for only the largest IAWs in each shock ramp. The largest correlation is between $|E_{xy}|$ and n_2/n_1 (seen in Fig. 2), consistent with larger shock strengths resulting in larger cross-field currents which may provide free energy for wave generation. A slightly weaker correlation is seen between $|E_{xy}|$ (mV/m) and M_f. Similar correlations were seen for the other Mach numbers. No correlation between T_e/T_i and wave amplitude was observed. Polarization vectors for IAWs are consistent with a cross-field current source. These waves produced $\eta_{\mathrm{IA}} = \nu/(\epsilon_o \omega_{\mathrm{pe}}^2)$ [33] ~1–856 $\Omega \cdot$ m (low end estimate assuming $T_e \gg T_i$) [34], which are $\sim 10^7$ times greater than classical estimates. These results are consistent with the theory that wave-particle interactions are important for dissipation at subcritical shocks [13,14].

The results of this study are consistent with previous studies suggesting IAW dominance in the ramp regions of shock waves [17–20]. Previous studies have also addressed questions about the typical solar wind conditions ($T_e \sim T_i$) suggesting temperature gradients and oblique propagation of the waves with respect to the ambient magnetic field improve the conditions necessary for IAW generation [12,19,20]. This study has provided the first statistical results on waveforms in IP shock ramps. Also previous studies have not distinguished the relative amplitudes (i.e., large vs small in this study) of wave modes in each region. The separation of TDS samples (by region and amplitude) illuminated an apparent amplitude dependence on shock strength, M_f, and region of occurrence. Although this study has provided new insights into the microphysics of IP shocks, further investigation is needed to gain a more fundamental understanding of wave phenomena and dissipation at IP shocks. Future studies will examine particle distributions for evidence of ion reflection and beam features.

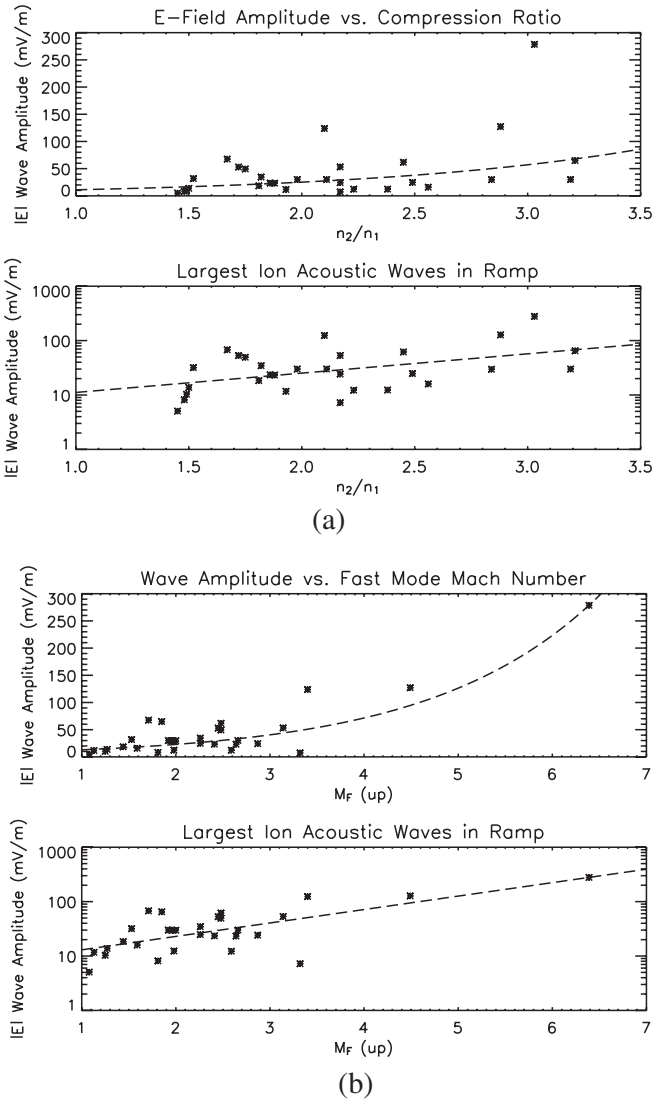

FIG. 2. Correlation plots for the largest IAWs in the ramp regions of 33 IP shocks. (a) Wave amplitude versus the compression ratio (n_2/n_1), and (b) fast Mach number. The dotted line corresponds to the exponential of the fit line defined in the upper left corner of each plot. The top panel is the data plotted on linear axes while the bottom panel has the y axis on a logarithmic scale.

The authors would like to acknowledge J. R. Wygant for useful discussions of shock physics. We would like to thank J. Woodroffe for technical support in IDL and LaTeX. We thank R. Lin (3DP), K. Ogilvie (SWE), and R. Lepping (MFI) for the use of data from their instruments. We would also like to thank P. Schroeder for technical help with the 3DP software and analysis.

*Present address: Princeton University, Princeton, New Jersey 08544, USA.

[1] S. D. Bale *et al.*, J. Geophys. Res. **102**, 11 281 (1997).
[2] S. D. Bale *et al.*, Geophys. Res. Lett. **25**, 2929 (1998).
[3] S. D. Bale *et al.*, Astrophys. J. **575**, L25 (2002).
[4] A. J. Hull *et al.*, Geophys. Res. Lett. **33**, L15 104 (2006).
[5] P. J. Kellogg *et al.*, J. Geophys. Res. **104**, 17 069 (1999).
[6] R. J. Fitzenreiter *et al.*, J. Geophys. Res. **108**, 1415 (2003).
[7] D. A. Gurnett, F. M. Neubauer, and R. Schwenn, J. Geophys. Res. **84**, 541 (1979).
[8] R. A. Hess *et al.*, J. Geophys. Res. **103**, 6531 (1998).
[9] G. Thejappa and R. J. MacDowall, Astrophys. J. **544**, L163 (2000).
[10] J. P. Edmiston and C. F. Kennel, J. Plasma Phys. **32**, 429 (1984).
[11] Charles F. Kennel, J. Geophys. Res. **92**, 13 427 (1987).
[12] M. F. Thomsen *et al.*, J. Geophys. Res. **90**, 137 (1985).
[13] S. Matsukiyo and M. Scholer, J. Geophys. Res. **111**, A06 104 (2006).
[14] N. Shimada and M. Hoshino, Astrophys. J. **543**, L67 (2000).
[15] C. Cattell *et al.*, Geophys. Res. Lett. **29**, 1065 (2002).
[16] C. Cattell *et al.*, J. Geophys. Res. **110**, A01 211 (2005).
[17] D. A. Gurnett *et al.*, J. Geophys. Res. **84**, 2029 (1979).
[18] T. G. Onsager *et al.*, J. Geophys. Res. **94**, 13 397 (1989).
[19] K. Akimoto and D. Winske, J. Geophys. Res. **90**, 12 095 (1985).
[20] S. A. Fuselier and D. A. Gurnett, J. Geophys. Res. **89**, 91 (1984).
[21] M. M. Mellott, *Geophys. Monograph Ser* (American Geophysical Union, Washington, DC, 1985), Vol. 35.
[22] R. E. Ergun *et al.*, Phys. Rev. Lett. **81**, 826 (1998).
[23] J. R. Franz *et al.*, J. Geophys. Res. **110**, A09 212 (2005).
[24] J. S. Pickett *et al.*, Nonlin. Proc. Geophys. **11**, 183 (2004).
[25] J. D. Williams *et al.*, Geophys. Res. Lett. **32**, L17 103 (2005).
[26] C. Cattell *et al.*, Geophys. Res. Lett. **26**, 425 (1999).
[27] J.-L. Bougeret *et al.*, Space Sci. Rev. **71**, 231 (1995).
[28] M. H. Farris, C. T. Russell, and M. F. Thomsen, J. Geophys. Res. **98**, 15 285 (1993).
[29] R. P. Lepping *et al.*, Space Sci. Rev. **71**, 207 (1995).
[30] J. C. Kasper, http://space.mit.edu/home/jck/shockdb/shockdb_files/.
[31] R. P. Lin *et al.*, Space Sci. Rev. **71**, 125 (1995).
[32] K. W. Ogilvie *et al.*, Space Sci. Rev. **71**, 55 (1995).
[33] $\nu = \omega_{\rm pe}\epsilon_o\delta E^2/(2nK_BT_e)$, where δE^2 is the electric field wave amplitude and $\omega_{\rm pe}$ is the electron plasma frequency.
[34] C. E. J. Watt *et al.*, Geophys. Res. Lett. **29**, 1004 (2002).